# Empirical Correction of XBT Data

M. Hamon, Gilles Reverdin, Pierre-Yves Le Traon

# Empirical Correction of XBT Data

M. HAMON

*Laboratoire d'Océanographie Spatiale, IFREMER, Plouzané, France*

G. REVERDIN

*LOCEAN, IPSL, CNRS/IRD/MNHN/UPMC, Paris, France*

P.-Y. LE TRAON

*Laboratoire d'Océanographie Spatiale, IFREMER, Plouzané, France*

(Manuscript received 10 August 2011, in final form 23 January 2012)

ABSTRACT

The authors use a collocation method between XBT and CTD/Ocean Station Data (OSD; including bottle cast and low-resolution CTD) from World Ocean Database 2005 (WOD2005) to statistically correct the XBT fall rate. An analysis of the annual median bias on depth shows that it is necessary to apply a thermal correction, a second-order correction on the depth, as well as a depth offset representing measurement errors during XBT deployment. Data were separated into several categories: shallow and deep XBTs and below or above 10°C of vertically averaged ocean temperatures (in the top 400 m). Also, XBT measurements in the western Pacific between 1968 and 1985 were processed separately because of large regional biases. The estimated corrections deviate from other published estimates with some large variations in time of both linear and curvature terms in the depth corrections, and less time variation of the temperature correction for the deep XBTs. This analysis of heat content derived from corrected XBTs provides at first order a similar variability to other estimates from corrected XBTs and mechanical bathythermographs (MBTs). It shows a fairly prominent trend in 0–700-m ocean heat content of $0.39 \times 10^{22}$ J yr$^{-1}$ between 1970 and 2008.

## 1. Introduction

Identifying and quantifying the changes in ocean heat content (OHC) is one of the most important research areas for the international oceanographic community. Because of its heat capacity, much larger than the other elements of the climate system, it is estimated that the oceans have absorbed more than 80% of the earth's warming due to the anthropogenic increase of greenhouse gas concentration (Levitus et al. 2001, 2005). In the last few years, many studies have tried to accurately determine the evolution of the global ocean heat content (e.g., Gouretski and Koltermann 2007; Wijffels et al. 2008; Levitus et al. 2009). These studies identified systematic differences between the different instruments used to collect ocean temperature profiles that need to be corrected. Since 1966, expendable bathythermographs (XBTs) mostly launched from ships, have been used to measure the upper-ocean's temperature, and constitute the most important source of upper-ocean data between the late 1960s and 2000. The XBT system does not directly measure depth. The accuracy of the depth associated with each temperature depends on an equation that converts the time elapsed since the probe entered the water to depth.

We will not review in detail the issues with the determination of this equation, which can be found in Hanawa et al. (1995) for early work and in Gouretski and Reseghetti [2010 (GR10)] for a more recent review. The parabolic character of the fall rate equation was initially validated by the observation of the fall of a probe in a freshwater tank at a homogeneous temperature. The linear term is a terminal velocity of the instrument and the second-order term is there to take into account mass changes of the probes as the wire is spun during its fall. It has been known since the early uses of the probes that the fall rate should depend on the seawater physical characteristics (e.g.,

*Corresponding author address:* Gilles Reverdin, LOCEAN, IPSL, CNRS/IRD/MNHN/UPMC, 4 Place Jussieu, 75252 Paris, France.
E-mail: gilles.reverdin@locean-ipsl.upmc.fr

DOI: 10.1175/JTECH-D-11-00129.1

a dependency on the viscosity–temperature–density of seawater; Thadathil et al. 2002; Kizu et al. 2011). It has also been suggested early on that the assumption of a terminal velocity might not be always correct, in particular in the surface layer, and that this, compounded with time constant issues, can result in a depth offset [although the determination of this depth offset is not straightforward, as discussed by DiNezio and Goni (2010), as it depends on many parameters hardly known and probably very variable]. The weight and hydrodynamic characteristics of the probe–wire are known to strongly influence the fall rate equation. Seaver and Kuleshov (1982), for example, indicate that a weight uncertainty of 2% could induce 8.8 m of depth error at 750 m. GR10 finds significant weight variations for probes manufactured after 1992 and there are strong suggestions based on dedicated comparisons done during cruises that the characteristics of the probes have changed in time [Hanawa et al. (1995) mostly late 1990–early 1990 data compared to DiNezio and Goni (2010) or Reverdin et al. (2009) for early 2000s data] and between manufacturers (e.g., Kizu et al. 2011). Different fall rate equations might also have been used to report the XBT profiles in the databases, adding confusion to the accuracy of the profiles. That the depth estimates have resulted in time-dependent biases dependent on the probe model is, for example, illustrated by comparison of the final reported depth to bathymetry on the shelves or continental slopes (Good 2011).

There are also subtle issues of temperature biases (associated with the probes, the electronics, circuitry, A/C converter, etc.; e.g., Roemmich and Cornuelle 1987) that have not been so well documented (Reseghetti et al. 2007; Reverdin et al. 2009). Usually, these biases were shown to have little dependence on depth, although some systems have been known to result in a large bowing of the profiles at depth, and thus a depth-dependent bias. Furthermore, it is possible that other errors are left in the database, even after quality control, for example, erroneously warm portions of the profiles after the wire has touched the hull or when it is otherwise stretched (see summary in GR10), both happening more commonly near the end of the profiles and that could result in average depth-dependent temperature biases.

These different issues with the data of XBTs in the databases explain why a large variety of approaches have been used to address the data biases, since it has been known that they contributed to anomalous low-frequency variability [e.g., the artificial ''global'' heat content increase of the 1970s or the recent problems identified in Willis et al. (2009)].

Gouretski and Koltermann (2007) used an ocean climatology based on high-quality data [conductivity–temperature–depth (CTD) and Nansen casts] to identify biases in XBT observations. They found a positive bias by 0.2°–0.4°C on average with some variations from year to year. Based on this study and further comparisons between data types, Wijffels et al. [2008 (W08)] proposed a yearly multiplicative correction factor on the depth. More recently, Levitus et al. (2009) used a simpler temperature correction, subtracting from all XBTs the annual median temperature bias obtained when comparing with the CTD climatology. Ishii and Kimoto (2009) estimated a new fall rate equation for each year, separating different kinds of XBTs. GR10 proposed a new correction for profiles in the World Ocean Database 2005 (WOD2005) using an average depth correction (but latitude dependent) added to a time-dependent temperature offset. Other interesting examples of statistical corrections of the temperature profile data in recent years can be found in DiNezio and Goni (2010), based on comparison with Argo float data that combine temperature biases and changes in the fall equation involving both offsets and a change in the quadratic fall rate equation.

These different approaches result in a fairly comparable reconstruction of vertically integrated heat content (IHC) variability from WOD2005 data. On the other hand, because of very different profiles of corrections, they might differ in the vertical structure of the changes. Thus, there is still a need for further studies of the biases in the historical datasets, so that the different types of data can be combined more optimally. Here, we provide a comparison of the different corrections, resulting in an alternative correction. The choice we made was applying a time-dependent but depth-independent temperature correction based on comparisons in the near-surface layer, and then correcting the depths at which the data are reported with a time-dependent correction. This entails two steps:

1) correction of the thermal bias:

$$T_{\text{cor}} = T_{\text{XBT}} - T_{\text{off}}(z), \tag{1}$$

where $T_{\text{XBT}}$ is the original XBT temperature and $T_{\text{off}}(z)$ is a specified temperature offset profile, and

2) correction of the depth bias:

$$Z_{\text{true}} = Z_{\text{xbt}}(1 - A - BZ_{\text{xbt}}) - Z_{\text{off}}, \tag{2}$$

where $Z_{\text{xbt}}$ is the original reported depth, $Z_{\text{off}}$ is a specified depth offset, and $A$ and $B$ are the specified terms for the linear and quadratic corrections.

A major difference with GR10 is that the two steps are done independently, and thus, to provide a significant reduction of the biases, all the coefficients in Eqs. (1) and (2) have to be time-dependent (whereas only $T_{\text{off}}$ is

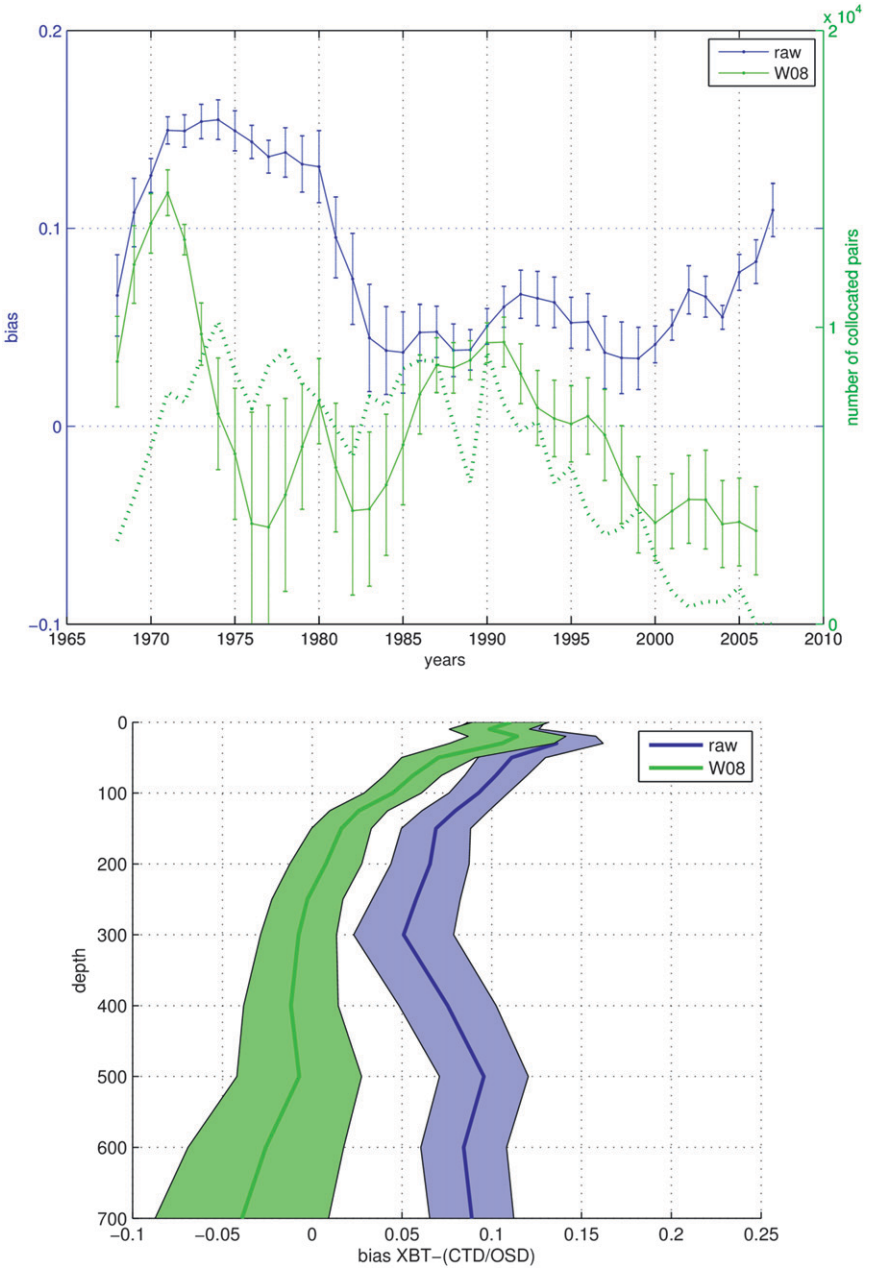


FIG. 1. The XBT − CTD 0–700-m median temperature bias in uncorrected data (blue) and in corrected W08 (green). (top) Vertical integral between 0 and 700 m [median value (curve) with vertical standard deviation (bars)]. The number of yearly collocated pairs is indicated with the green dotted line (right axis). (bottom) Vertical profiles of median raw bias and of median bias after correction by W08 averaged over the study period (average curve and colored range within one std dev). Units: °C.

time-dependent in GR10). On the other hand, the spatial dependency of the depth correction is more crudely taken into account in this approach than in GR10.

In section 2, we will present the data and the collocation method; in section 3, we will review what W08 depth corrections imply in terms of residual biases. Then, in section 4, we will discuss the thermal correction, compare it with GR10, and discuss the remaining residuals. In section 5 we will discuss the depth corrections, before presenting the resulting heat content time series with the corrections adopted (section 6) and the conclusions (section 7).

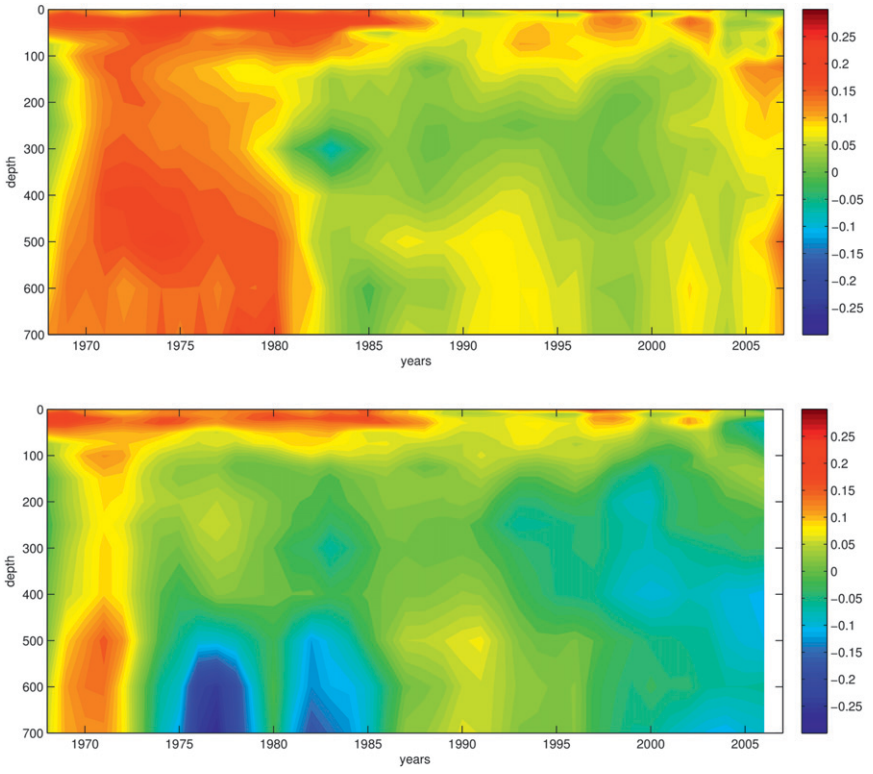


FIG. 2. Evolution of XBT − CTD (top) median raw bias and (bottom) corrected by W08 as a function of depth and time. Units: °C.

## 2. Data and collocation method

In the current study we used temperature profiles of the World Ocean Database 2005 where profiles have been interpolated to standard levels. The ocean was subdivided into 16 vertical levels from the surface to 700-m depth. We used profiles that have been processed when identification was possible using the correction Hanawa et al. (1995, hereafter H95). Instead of using two climatologies, one constructed with CTD and bottles profiles and the other with XBT profiles, we used a collocation method to compare instruments. For each XBT, we selected all CTD and Ocean Station Data (OSD) geographically distant by less than 1° of latitude and 2° of longitude and a time lag less than 15 days. Then, we computed a reference profile as the median of all CTD and OSD profiles selected in the region of collocation. The bias profile is calculated by subtracting this reference profile from the XBT profile. We found that many comparisons corresponded to situations with an XBT deployed over the deep ocean and CTD stations over the shelf or the continental slope. Thus to avoid potential biases resulting from cross-shelf fronts, we also ensure that ocean depth where the XBTs have been deployed is larger than 150 m and does not differ by more than 500 m from where CTDs have been deployed (we discuss this added condition in section 4). Finally we rejected collocated XBT and CTD profiles for which the resulting vertically averaged bias was more than 1°C. This method allows us to retain about $10^4$ profiles per year between the years 1968 and 2007 (Fig. 1). Following Levitus et al. (2009), the median rather than arithmetic average was used, as it reduces the influence of outliers. It is important to realize that this median temperature bias (its vertical average in Fig. 1) contributes only a small portion (on the order of 1%–2% near 300–400-m depth) of the total variance in the individual XBT–CTD profiles of temperature difference, which is dominated by the time–space variability. However, uncertainties in the median bias profiles that are considered in this study are small enough because of the inclusion of a large number of individual bias profiles (Fig. 1).

First, we estimate a temperature offset $T_{\text{off}}$ by selecting profiles with very weak thermal gradients between 10 and 30 m (cf. section 4). After removal of the temperature offset [Eq. (1)] to the data, we adjust the depth indicated by the original fall rate [Eq. (2)]. We compute a depth bias at each standard level with the first-order approximation as

$$\delta Z = (T_{\text{CTD}} - T_{\text{cor}}) dZ/dT_{\text{cor}}, \tag{3}$$

where $dZ/dT_{\text{cor}}$ is a local estimate of the vertical temperature gradient based on the XBT uncorrected depth

TABLE 1. Thermal offset (°C) as a function of time for XBTD (ToffsetD) and XBTS (ToffsetS), and western Pacific XBTs (ToffsetWP; north of 20°S and west of 180°E).

| Year | ToffsetD | ToffsetS | ToffsetWP |
|---|---|---|---|
| 1968 | 0.049 | 0.084 | −0.006 |
| 1969 | 0.052 | 0.083 | 0.002 |
| 1970 | 0.051 | 0.080 | 0.020 |
| 1971 | 0.067 | 0.084 | 0.036 |
| 1972 | 0.081 | 0.087 | 0.043 |
| 1973 | 0.090 | 0.087 | 0.049 |
| 1974 | 0.098 | 0.091 | 0.055 |
| 1975 | 0.096 | 0.098 | 0.056 |
| 1976 | 0.089 | 0.105 | 0.051 |
| 1977 | 0.079 | 0.112 | 0.051 |
| 1978 | 0.070 | 0.118 | 0.055 |
| 1979 | 0.059 | 0.121 | 0.050 |
| 1980 | 0.059 | 0.119 | 0.047 |
| 1981 | 0.061 | 0.109 | 0.039 |
| 1982 | 0.062 | 0.099 | 0.031 |
| 1983 | 0.054 | 0.089 | 0.019 |
| 1984 | 0.056 | 0.082 | 0.014 |
| 1985 | 0.056 | 0.077 | 0.004 |
| 1986 | 0.053 | 0.077 | |
| 1987 | 0.049 | 0.073 | |
| 1988 | 0.059 | 0.062 | |
| 1989 | 0.056 | 0.049 | |
| 1990 | 0.049 | 0.034 | |
| 1991 | 0.047 | 0.021 | |
| 1992 | 0.051 | 0.011 | |
| 1993 | 0.051 | 0.009 | |
| 1994 | 0.059 | 0.011 | |
| 1995 | 0.074 | 0.015 | |
| 1996 | 0.087 | 0.014 | |
| 1997 | 0.090 | 0.011 | |
| 1998 | 0.093 | 0.005 | |
| 1999 | 0.093 | 0.000 | |
| 2000 | 0.082 | −0.014 | |
| 2001 | 0.066 | −0.036 | |
| 2002 | 0.058 | −0.020 | |
| 2003 | 0.048 | 0.006 | |
| 2004 | 0.037 | 0.018 | |
| 2005 | 0.031 | 0.027 | |
| 2006 | 0.032 | 0.043 | |
| 2007 | 0.029 | 0.008 | |

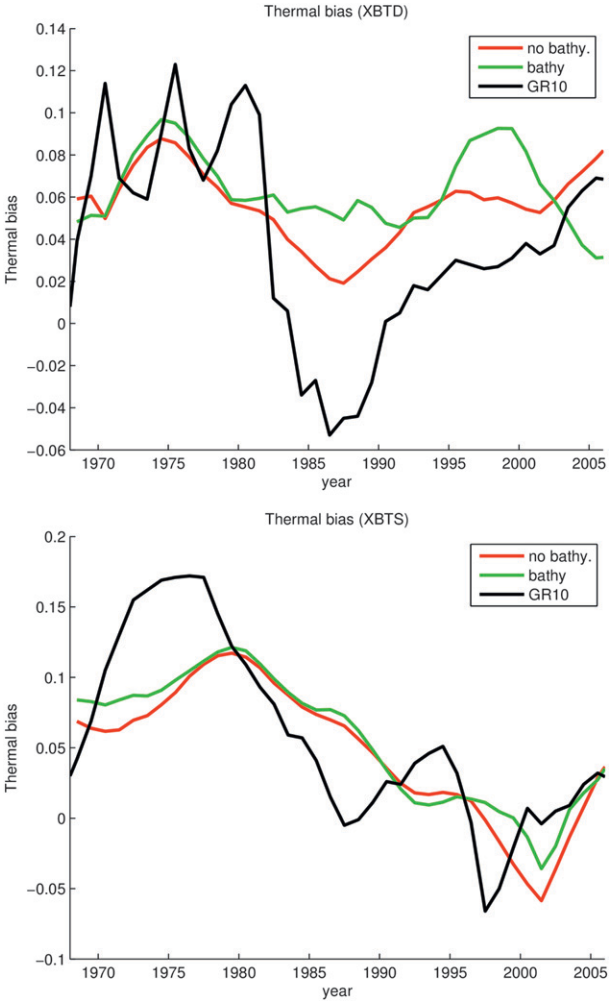


FIG. 3. Median XBT − CTD thermal bias for (top) XBTD and (bottom) XBTS. Thermal bias observed from collocated data without bathymetry criterion is represented by the red line, with the bathymetry criterion by the green line, and the thermal offset of GR10 by the black line. Units: °C.

profile. Then we correct the depth estimates $Z_{xbt}$ by the median $\langle \delta Z \rangle$ of these depths, and to get temperatures with this new set of depths, we linearly interpolate the XBT temperature profile to the standard levels:

$$T = T_{cor} + \langle \delta Z \rangle dT_{cor}/dZ. \quad (4)$$

However, because in Eq. (3) the gradient term is calculated from the uncorrected depth estimates of the XBT profiles, it is actually also shifted vertically to the real gradient at that depth. Thus it is necessary to iterate with the new "vertically shifted" temperature profile until convergence is reached when the corrected XBT gradients will be statistically similar to the ones from the CTDs.

Once the median depth bias $\langle \delta Z \rangle$ vertical profile is obtained at the standard levels, we estimate the three coefficients in the parabolic depth correction Eq. (2) by a linear least squares method.

## 3. Test of the W08 correction

The W08 correction is a linear correction where the "true" estimated XBT depth $Z_{true}$ is computed from the depth $Z$ given with the original fall rate:

$$Z_{true} = Z_{xbt}(1 - A). \quad (5)$$

W08 separated the deep XBT profiles (hereafter called XBTD) into those reaching a depth greater than 500 m

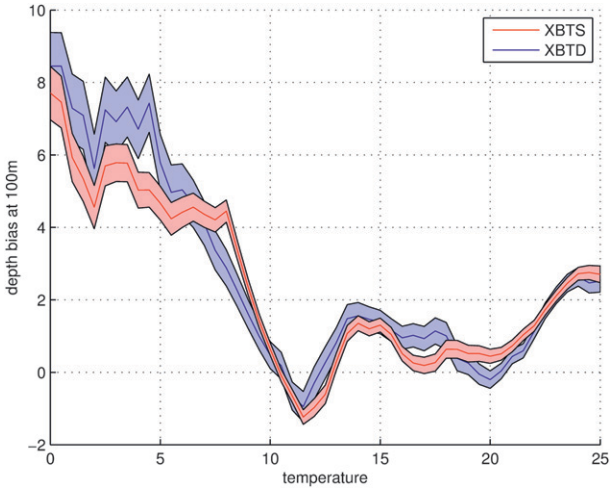


FIG. 4. Median XBT − CTD depth bias at 100-m depth as a function of the integrated temperature between 0- and 200-m depth for XBTS (red) and XBTD (blue). The width provides the range of the ±one std dev of the uncertainty (std dev divided by the square root of the number of selected pairs). Units: °C.

(in standard levels), which are predominantly profiles from T7 or Deep Blue instruments and the others, shallow XBT profiles (hereafter called XBTS), which are predominantly from T4–T6 instruments. On average, W08 note a depth error near 400 m of 10 m for XBTS and half that for XBTD profiles.

We first applied the W08 correction to our collocated profiles. Figure 1 shows the yearly raw and W08 corrected median bias averaged vertically as a function of year, and the average bias profile. According to Gouretski and Koltermann (2007) and Wijffels et al. (2008) there is a positive bias between vertically averaged XBT temperature and high-quality data like CTD and OSD. This median bias varies with the year of deployment of the XBT. It varies between 0.2° and 0.1°C during the end of the 1960s until the beginning of the 1980s. Then the bias stabilizes around 0.05°C. Moreover, this evolution agrees with the results of Levitus et al. (2009). This vertically averaged bias is partially corrected by W08 corrections (Fig. 1).

The 1-yr median bias function of depth is not uniformly reduced while applying the W08 correction (Fig. 2). Obviously the linear depth equation correction cannot correct the surface bias. Sometimes, it can also be too large and induce a negative bias at some depths (Fig. 2). The comparison thus suggests that a linear depth correction is not sufficient to properly reduce the observed biases (as also stated by GR10).

## 4. Temperature correction

Comparing neighboring XBT and CTD–OSD profiles in the upper mixed layer, we usually observe a positive thermal bias between 10 and 30 m. Following GR10, we selected close-by profiles with a weak temperature gradient in this upper layer (less than 0.0025°C $m^{-1}$). This criterion guarantees that the observed bias is more likely to be related to a temperature error than to incorrect estimation of depth (this was also checked after the corrections on the depth of the XBT profiles of section 5, with little difference in the results). We also restricted the difference in ocean depth of collocated profiles to 500 m.

As we did not find significant differences in this temperature bias related to sea surface temperature (between warm and cold seas), we decided to take into account only two categories (XBTS and XBTD) to estimate more robustly the temperature bias $T_{off}$ (Table 1). The thermal offset associated with XBTS is largely positive between 1968 and 1985 (0.096°C on average) and is close to 0° afterward (Fig. 3). The thermal bias of XBTD varies less. A first maximum is reached between 1970 and 1980

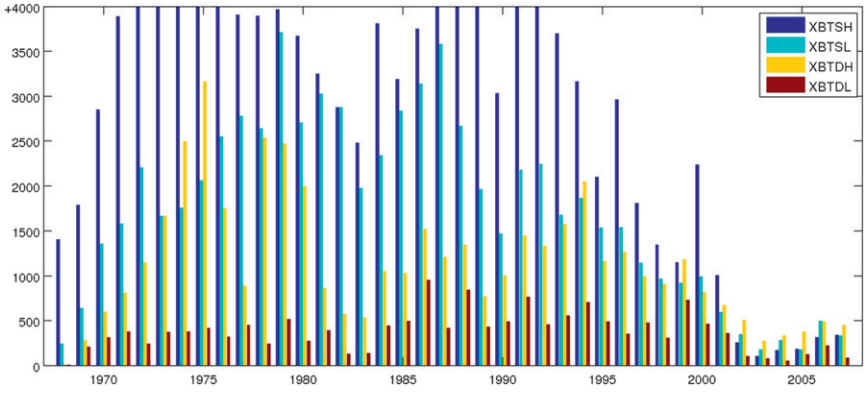


FIG. 5. Number of collocated pairs for the four classes of XBT as a function of year. XBTS(D)H–XBTS(D)L correspond to shallow (deep) XBTs deployed in high and low temperatures, respectively.

TABLE 2. Coefficients of the parabolic depth Eq. (2) and depth offset for XBTD deployed in low- (DL) and high- (DH) temperature waters ($A$: nondimensional, $B$: in $m^{-1}$, and Offset: for $Z_{off}$ in m).

| Year | $B_{DL}$ | $A_{DL}$ | $Offset_{DL}$ | $B_{DH}$ | $A_{DH}$ | $Offset_{DH}$ |
|---|---|---|---|---|---|---|
| 1968 | 0.052 | −0.000 078 | 1.0 | −0.054 | 0.000 006 | 0.9 |
| 1969 | 0.024 | −0.000 016 | 1.5 | −0.039 | 0.000 046 | 0.9 |
| 1970 | −0.006 | 0.000 040 | 1.3 | −0.025 | 0.000 066 | 0.9 |
| 1971 | −0.014 | 0.000 038 | 1.7 | −0.010 | 0.000 039 | 0.8 |
| 1972 | −0.008 | −0.000 004 | 2.1 | 0.015 | −0.000 006 | 0.6 |
| 1973 | 0.021 | −0.000 082 | 2.4 | 0.023 | −0.000 021 | 0.5 |
| 1974 | 0.062 | −0.000 151 | 2.7 | 0.008 | 0.000 003 | 0.5 |
| 1975 | 0.075 | −0.000 137 | 2.9 | 0.001 | 0.000 016 | 0.6 |
| 1976 | 0.052 | −0.000 049 | 2.9 | 0.021 | −0.000 015 | 0.4 |
| 1977 | 0.018 | 0.000 037 | 2.5 | 0.048 | −0.000 057 | 0.1 |
| 1978 | −0.004 | 0.000 070 | 1.8 | 0.046 | −0.000 054 | 0.0 |
| 1979 | −0.004 | 0.000 062 | 1.3 | 0.029 | −0.000 021 | 0.0 |
| 1980 | 0.026 | 0.000 025 | 1.3 | 0.019 | 0.000 002 | 0.1 |
| 1981 | 0.026 | 0.000 019 | 1.3 | 0.017 | −0.000 004 | 0.2 |
| 1982 | −0.070 | 0.000 102 | 0.9 | 0.019 | −0.000 026 | 0.4 |
| 1983 | −0.156 | 0.000 167 | 0.4 | −0.009 | 0.000 013 | 0.6 |
| 1984 | −0.145 | 0.000 118 | 0.6 | −0.048 | 0.000 071 | 0.7 |
| 1985 | −0.084 | 0.000 006 | 1.4 | −0.039 | 0.000 054 | 0.9 |
| 1986 | −0.037 | −0.000 053 | 2.3 | −0.012 | 0.000 015 | 1.2 |
| 1987 | −0.021 | −0.000 033 | 2.9 | −0.005 | 0.000 003 | 1.6 |
| 1988 | −0.018 | −0.000 003 | 3.1 | −0.015 | 0.000 014 | 1.9 |
| 1989 | −0.025 | 0.000 014 | 2.8 | −0.022 | 0.000 022 | 1.8 |
| 1990 | −0.027 | 0.000 016 | 2.4 | −0.010 | 0.000 011 | 1.6 |
| 1991 | −0.031 | 0.000 025 | 2.2 | −0.008 | 0.000 012 | 1.4 |
| 1992 | −0.026 | 0.000 025 | 2.0 | −0.006 | 0.000 016 | 1.0 |
| 1993 | −0.003 | 0.000 001 | 1.8 | 0.006 | 0.000 004 | 0.6 |
| 1994 | 0.001 | 0.000 003 | 1.7 | 0.006 | 0.000 000 | 0.4 |
| 1995 | −0.030 | 0.000 038 | 2.0 | −0.006 | 0.000 007 | 0.4 |
| 1996 | −0.068 | 0.000 066 | 2.5 | −0.009 | 0.000 006 | 0.6 |
| 1997 | −0.073 | 0.000 040 | 3.2 | −0.001 | −0.000 006 | 0.9 |
| 1998 | −0.063 | −0.000 012 | 3.9 | −0.014 | −0.000 000 | 1.5 |
| 1999 | −0.080 | −0.000 004 | 4.6 | −0.041 | 0.000 026 | 1.9 |
| 2000 | −0.107 | 0.000 043 | 4.8 | −0.033 | 0.000 023 | 1.8 |
| 2001 | −0.131 | 0.000 091 | 4.2 | 0.002 | −0.000 008 | 1.3 |
| 2002 | −0.132 | 0.000 110 | 3.2 | 0.013 | −0.000 014 | 0.8 |
| 2003 | −0.073 | 0.000 060 | 1.8 | 0.004 | 0.000 002 | 0.6 |
| 2004 | 0.010 | −0.000 031 | 0.6 | 0.001 | 0.000 001 | 0.4 |
| 2005 | 0.059 | −0.000 109 | 0.1 | 0.011 | −0.000 022 | 0.4 |
| 2006 | 0.071 | −0.000 138 | 0.6 | 0.029 | −0.000 041 | 0.5 |
| 2007 | 0.012 | −0.000 011 | 2.2 | 0.033 | −0.000 032 | 0.7 |

(0.076°C on average), which decreases during the 1980s and becomes the maximum again at the end of the 1990s (0.086°C on average between 1995 and 2000).

XBTD (and even T4 XBTs) are more often deployed in the deep seas whereas the number of CTDs is at a maximum on the shelves. In continental slope regions where a large proportion of collocated profiles are, comparisons between XBT and CTD profiles can yield unrealistic biases. As shown in Fig. 3, the criterion of similar ocean depths has a large impact on the calculation of the thermal offset, especially for XBTD for the period 1985–2000. It appears that including CTDs deployed on continental shelves induced an artificial thermal offset. The time histories of the thermal corrections we find for XBTS and XBTD are rather different, something we do not have an explanation for (this is also commented upon in GR10).

We find that the thermal bias we estimate for XBTD differs after 1982 from the one reported in GR10. In GR10, the thermal offset becomes largely negative whereas our observed bias is much more constant and positive for the whole study period. For XBTS, on the other hand, the low-frequency evolution we find presents some similarities with the one in GR10, with a maximum during the 1970s, a decrease until the end of the 1990s, and a slight increase afterward. However, the correction for a given year can be quite different, and the total range of corrections here is only half the one in GR10.

Altogether, we also find that just correcting a thermal bias reduces the average biases more efficiently than applying a linear depth correction scheme as in W08. However, it leaves a time-varying vertically averaged temperature bias, and thus is not appropriate for heat content variability estimations. Furthermore, the rms deviation of vertical variations in the annual bias profile is the same as in the raw data. This is usually better than with the W08 correction (Fig. 1), but is nonetheless still very large. Further discussion of the different ways to compare the data is provided in section 6.

## 5. The XBT depth correction

### *a. Temperature dependence of the depth correction*

We will try to refine the model of bias correction by examining in more detail the vertical and spatial structure of the XBT − CTD temperature difference, after removal of the thermal offset identified in 4.1. We will first comment on its sensitivity to the ocean temperature, separating XBTS and XBTD as done earlier. Such a dependency between depth bias and the temperature of the seawater where the probe had been deployed has been discussed earlier for different temperature ranges (Thadathil et al. 2002; Kizu et al. 2011). Figure 4 shows the depth bias at 100 m as a function of average temperature between 0 and 200 m for XBTS (in red) and XBTD (in blue) averaged over the study period. We notice an increase of the bias toward low temperatures, without finding a significantly different behavior between the two classes of XBTs (XBTS and XBTD). Thus Fig. 4 illustrates the need to process XBTs in categories of temperature, but at this particular depth, XBTS temperature offsets are not clearly different from the temperature offset in XBTD.

Whereas Fig. 4 suggests that fall rate depends continuously on temperature (viscosity), retaining only two

TABLE 3. Coefficients of the parabolic depth Eq. (2) and depth offset for XBTS deployed in low- (SL) and high- (SH) temperature waters ($A$: nondimensional, $B$: in $m^{-1}$, and Offset: for $Z_{off}$ in m).

| Year | $B_{SL}$ | $A_{SL}$ | $Offset_{SL}$ | $B_{SH}$ | $A_{SH}$ | $Offset_{SH}$ |
|---|---|---|---|---|---|---|
| 1968 | −0.018 | −0.000 109 | 3.4 | −0.033 | 0.000 100 | 2.4 |
| 1969 | −0.079 | 0.000 024 | 3.0 | −0.072 | 0.000 155 | 2.0 |
| 1970 | −0.053 | 0.000 014 | 3.0 | −0.070 | 0.000 146 | 2.1 |
| 1971 | 0.012 | −0.000 080 | 2.3 | −0.020 | 0.000 047 | 1.5 |
| 1972 | 0.073 | −0.000 165 | 1.7 | 0.027 | −0.000 032 | 1.0 |
| 1973 | 0.089 | −0.000 147 | 1.5 | 0.029 | −0.000 012 | 0.9 |
| 1974 | 0.071 | −0.000 069 | 1.6 | −0.006 | 0.000 062 | 1.2 |
| 1975 | 0.074 | −0.000 069 | 1.4 | −0.021 | 0.000 078 | 1.4 |
| 1976 | 0.096 | −0.000 137 | 1.0 | −0.003 | 0.000 027 | 1.3 |
| 1977 | 0.120 | −0.000 198 | 0.6 | 0.015 | 0.000 004 | 0.9 |
| 1978 | 0.123 | −0.000 216 | 0.4 | 0.005 | 0.000 034 | 0.6 |
| 1979 | 0.110 | −0.000 216 | 0.5 | −0.008 | 0.000 051 | 0.7 |
| 1980 | 0.097 | −0.000 222 | 0.7 | −0.014 | 0.000 063 | 0.9 |
| 1981 | 0.083 | −0.000 235 | 1.0 | −0.030 | 0.000 097 | 1.3 |
| 1982 | 0.071 | −0.000 250 | 1.1 | −0.041 | 0.000 114 | 1.6 |
| 1983 | 0.059 | −0.000 264 | 1.2 | −0.041 | 0.000 099 | 1.7 |
| 1984 | 0.041 | −0.000 245 | 1.3 | −0.034 | 0.000 072 | 1.8 |
| 1985 | 0.019 | −0.000 158 | 1.7 | −0.025 | 0.000 054 | 1.7 |
| 1986 | −0.014 | −0.000 039 | 2.2 | −0.032 | 0.000 056 | 1.6 |
| 1987 | −0.042 | 0.000 047 | 2.6 | −0.029 | 0.000 038 | 1.5 |
| 1988 | −0.046 | 0.000 067 | 2.7 | −0.019 | 0.000 013 | 1.3 |
| 1989 | −0.037 | 0.000 036 | 2.4 | −0.012 | 0.000 006 | 1.0 |
| 1990 | −0.034 | 0.000 010 | 2.2 | −0.006 | 0.000 009 | 0.8 |
| 1991 | −0.033 | −0.000 002 | 2.2 | 0.003 | −0.000 003 | 0.6 |
| 1992 | −0.035 | 0.000 003 | 2.4 | 0.012 | −0.000 018 | 0.5 |
| 1993 | −0.041 | 0.000 023 | 2.5 | −0.002 | 0.000 022 | 0.5 |
| 1994 | 0.036 | 0.000 009 | 2.3 | −0.020 | 0.000 069 | 0.7 |
| 1995 | −0.009 | −0.000 049 | 2.0 | −0.006 | 0.000 035 | 0.8 |
| 1996 | 0.015 | −0.000 083 | 1.8 | 0.023 | −0.000 056 | 0.8 |
| 1997 | −0.003 | −0.000 009 | 2.1 | 0.028 | 0.000 111 | 0.8 |
| 1998 | −0.051 | 0.000 141 | 2.8 | 0.003 | −0.000 082 | 1.1 |
| 1999 | −0.089 | 0.000 263 | 3.5 | −0.016 | −0.000 023 | 1.3 |
| 2000 | −0.093 | 0.000 295 | 3.7 | −0.007 | −0.000 004 | 1.3 |
| 2001 | −0.063 | 0.000 210 | 3.4 | 0.003 | −0.000 005 | 1.3 |
| 2002 | −0.008 | 0.000 044 | 3.1 | −0.036 | 0.000 061 | 1.9 |
| 2003 | 0.026 | 0.000 020 | 3.0 | −0.092 | 0.000 154 | 2.6 |
| 2004 | 0.014 | 0.000 113 | 2.7 | −0.085 | 0.000 184 | 2.4 |
| 2005 | 0.027 | 0.000 030 | 2.0 | −0.006 | 0.000 083 | 1.0 |
| 2006 | 0.070 | −0.000 138 | 0.9 | 0.082 | −0.000 102 | −0.1 |
| 2007 | 0.128 | −0.000 304 | −0.1 | 0.123 | −0.000 236 | −0.3 |

0–200-m averaged temperature classes is a practical first-order choice, as the computation of the depth bias requires a sufficient number of profiles to be robust (notice the relatively small number of comparisons at the lower temperatures in Fig. 5, which prevents us from subdividing further this temperature range). In practice, the two categories in vertically averaged temperature overlap to avoid discontinuities between profiles deployed in water close to 10°C: when computing the correction for the high-temperature class, we selected all XBTs deployed in water warmer than 8°C, whereas for the low-temperature class, we selected XBTs deployed in water colder than 12°C.

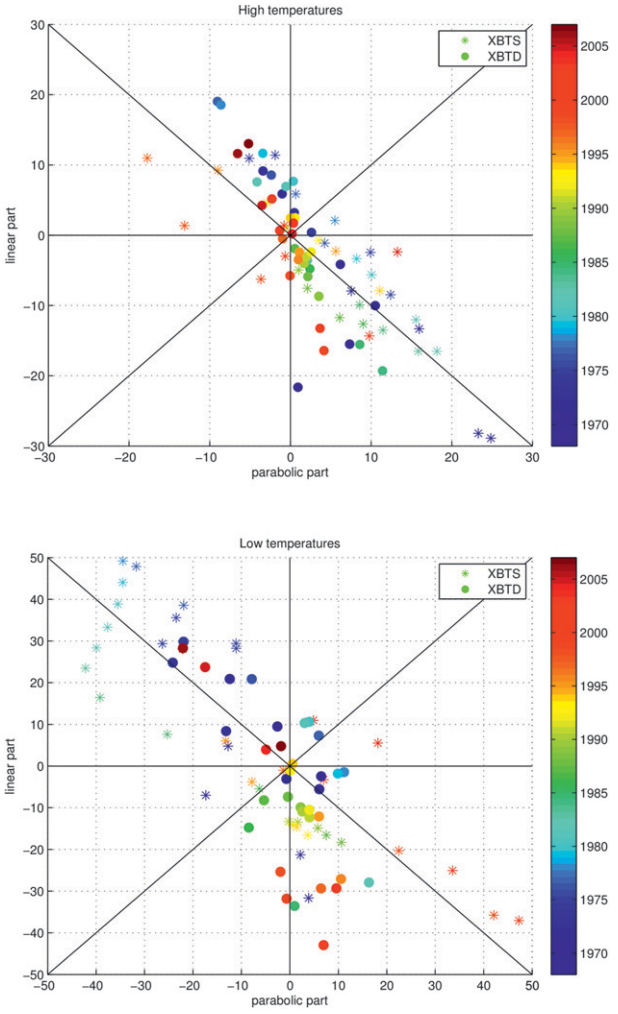


FIG. 6. Linear part ($A$) an a function of parabolic part ($BZ$) in Eq. (2) at $Z$ = 400-m depth for XBTS (large dots) and XBTD (stars). XBTs deployed at (top) high and (bottom) low temperatures. Years are indicated with the color bar.

### b. *Parabolic nature of the depth correction*

As in W08, the behavior of XBTS and XBTD is found to be different in the deeper part of the profile. This suggests that the collocated profiles are better corrected by a parabolic function than by a linear correction.

This parabolic character varies with years, geographical area, and the type of XBT. We thus computed a second-order correction with a least squares fitting process for each year of deployment and each class of XBT (Tables 2, 3). The depth bias also has a different behavior in the first meters of the probe fall. Between the surface and 30 m, the error deviates from its parabolic behavior, possibly because of the high variability of surface temperature added to the low vertical gradient in the surface mixed layer producing high variability in the calculated $dZ$ quantities.

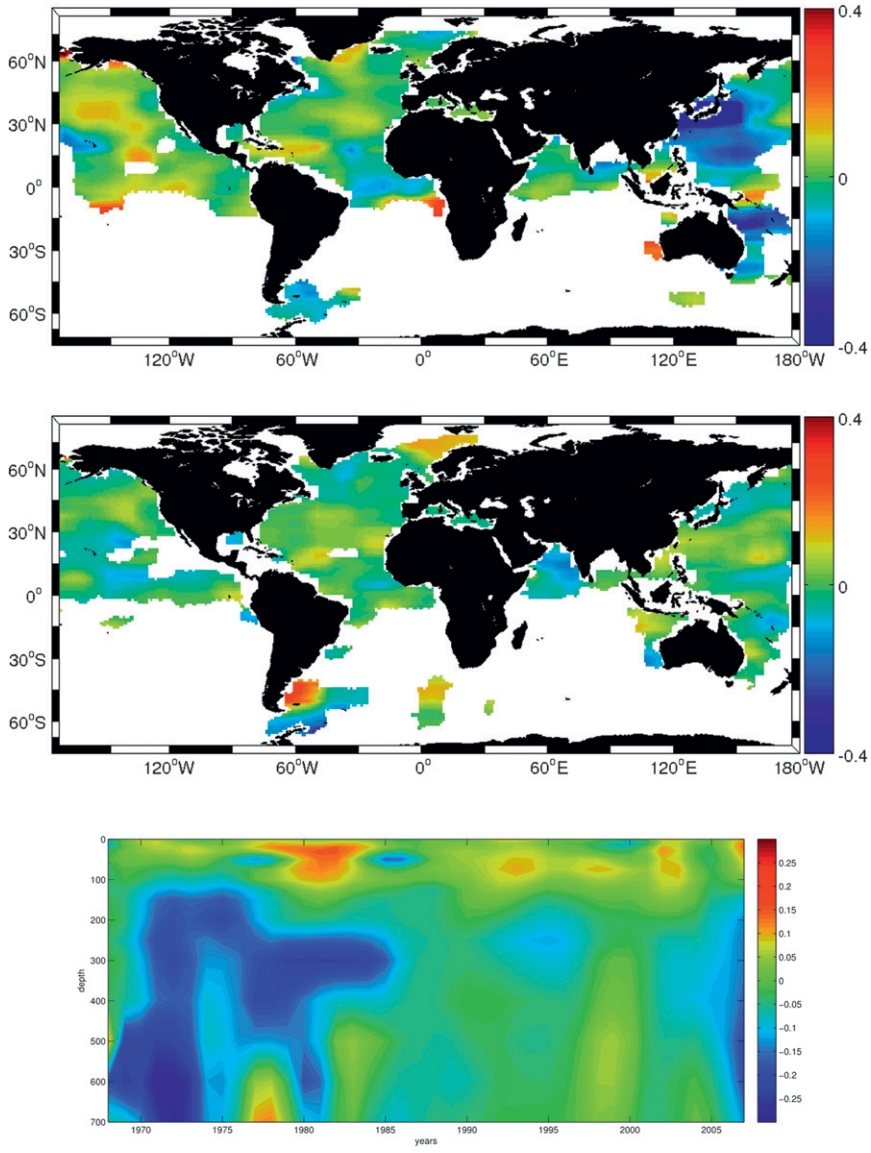


FIG. 7. Residual average bias in XBT − CTD temperature at 300 m (top) between 1968 and 1985 and (middle) between 1985 and 2007. (bottom) Evolution of XBT − CTD median bias in the western Pacific (the region is bounded by 180°E and 20°S). This corresponds to XBT data corrected by a global parabolic correction, as a function of depth and time. Units °C.

As suggested by earlier studies (see GR10), the depth correction equation is far from linear. Figure 6 represents the linear part $AZ_{\mathrm{xbt}}$ as a function of the parabolic part at 400-m depth $BZ^2_{\mathrm{xbt}}$ in Eq. (2) for XBTS (circles) and XBTD (stars) at high temperature (top panel) and at low temperature (bottom panel). Each sector represents a different behavior of the yearly median depth bias. At zero order, the two terms nearly compensate each other at that depth, and often seem rather positively correlated between low and high temperatures. However, between 1968 and 1980, the behavior of XBTS is clearly different with a positive parabolic part at low temperatures and a negative contribution at high temperatures. At high temperatures, the behaviors of the XBTS and XBTD fall rates are very different. In particular, until 1980 for XBTS, the parabolic part is positive and the linear part is negative, whereas it is the opposite for XBTD. Between 1985 and 1990, the behavior of the fitted bias deviates from other periods, in particular at the lower temperatures with both linear and parabolic parts being negative for XBTD. These differences of behavior justify the need to separate profiles for low and high temperatures.

TABLE 4. Coefficients of the parabolic depth Eq. (2) and depth offset for XBTD (DWP) and XBTS (SWP) deployed in the western Pacific Ocean ($A$: nondimensional, $B$: in $m^{-1}$, and Offset: $Z_{off}$ in m).

| Year | $B_{DWP}$ | $A_{DWP}$ | $Offset_{DWP}$ | $B_{SWP}$ | $A_{SWP}$ | $Offset_{SWP}$ |
|---|---|---|---|---|---|---|
| 1968 | −0.113 | 0.000 430 | 0.0 | 0 | 0 | 0 |
| 1969 | −0.090 | 0.000 320 | 0.1 | 0 | 0 | 0 |
| 1970 | −0.055 | 0.000 159 | 0.1 | 0 | 0 | 0 |
| 1971 | −0.035 | 0.000 078 | 0.1 | 0 | 0 | 0 |
| 1972 | −0.019 | 0.000 052 | −0.0 | −0.046 | 0.000 021 | −0.1 |
| 1973 | −0.011 | 0.000 047 | 0.0 | −0.013 | −0.000 023 | 0.3 |
| 1974 | −0.025 | 0.000 080 | 0.1 | −0.018 | 0.000 034 | 0.2 |
| 1975 | −0.024 | 0.000 091 | 0.1 | −0.015 | 0.000 097 | 0.2 |
| 1976 | −0.013 | 0.000 077 | 0.2 | −0.019 | 0.000 101 | 0.3 |
| 1977 | −0.001 | 0.000 032 | 0.5 | −0.019 | 0.000 039 | 0.6 |
| 1978 | −0.011 | 0.000 015 | 0.9 | −0.037 | 0.000 036 | 0.9 |
| 1979 | −0.029 | 0.000 048 | 1.2 | −0.054 | 0.000 078 | 1.0 |
| 1980 | −0.027 | 0.000 052 | 1.2 | −0.028 | 0.000 026 | 0.9 |
| 1981 | −0.025 | 0.000 046 | 1.2 | −0.015 | 0.000 024 | 0.8 |
| 1982 | −0.037 | 0.000 055 | 1.4 | −0.017 | 0.000 066 | 0.8 |
| 1983 | −0.059 | 0.000 083 | 1.5 | −0.008 | 0.000 041 | 0.7 |
| 1984 | −0.070 | 0.000 111 | 1.4 | −0.003 | 0.000 022 | 0.2 |
| 1985 | −0.056 | 0.000 103 | 1.1 | 0.009 | −0.000 004 | 0.7 |

### c. Depth offset

Without introducing a depth offset, the resulting temperature bias after temperature correction and parabolic depth correction is still positive in the surface layer. In this layer, the depth bias calculation involving the local gradient of temperature is not very accurate; but this also seems to correspond to a positive median depth bias that is not easily modeled by a parabolic function and thus is best considered to be a depth bias. The sources of this depth offset are very varied and the information that would be necessary to accurately model the XBT fall rate in the upper layer is not available. To overcome this lack of information we opt for an empirical fitting, proportionally adjusting the offset with the pre-corrected bias by the parabolic function. We used the yearly median depth bias between 30 and 100 m to statically correct the depth offset error. We chose to compute the offset in this thin layer because it corresponds to a compromise between the choice of a surface layer, where the effect of the offset would be most evident in the depth estimate, and a deeper layer with a large enough vertical temperature gradient:

$$Z_{off} = \langle \delta Z \rangle_{30-100}. \quad (6)$$

We note that the depth offset (Tables 2, 3) is usually positive and of a few meters with slightly larger values in low-temperature waters and around 2000. Those results are also consistent with Reverdin et al. (2009) for the period 1999–2007 for a subset of XBT data deployed during French research cruises, and with the results of GR10.

### d. Specific western Pacific case

After the global bias analysis by collocation, it is possible that residual biases may be identified regionally, as could happen because of sampling characteristics in the Kuroshio or Gulf Stream region, or because of regional processing or differences in the systems used. Measurements close to Japan and in the western Pacific basin (the northwest Pacific region bounded by 180°E and north of 20°S) show after the corrections a strong negative bias during the period 1968–85, in particular near 300 m (Fig. 7, top panel), but less afterward (Fig. 7, middle panel). This negative bias has a vertical profile and time history (Fig. 7, bottom panel), and implies that these XBTs are poorly corrected by the globally derived parabolic term. We were not able to establish fully the reason for this time-dependent regional anomaly (also commented on in W08). Because this is a large enough region, it has an impact on the global correction estimates, which we consider detrimental. Thus, we separated these regional profiles into another category, which increased the robustness of the correction estimated for the other data (Table 4). The coefficients $A$ and $B$ calculated for these particular XBTs are quite different from those calculated for the other classes, in particular for XBTD. The parabolic coefficient $B$ of the XBTD correction is largely positive in the first years and decreases until 1985, and the linear coefficient $A$ is strongly negative and increases with time. This behavior is specific to those regional XBTDs. Note also that the depth offset is much smaller for those XBTs than in other regions of the world. Furthermore, the temperature offset (Table 1; where it is not estimated separately for XBTS and XBTD, as the two

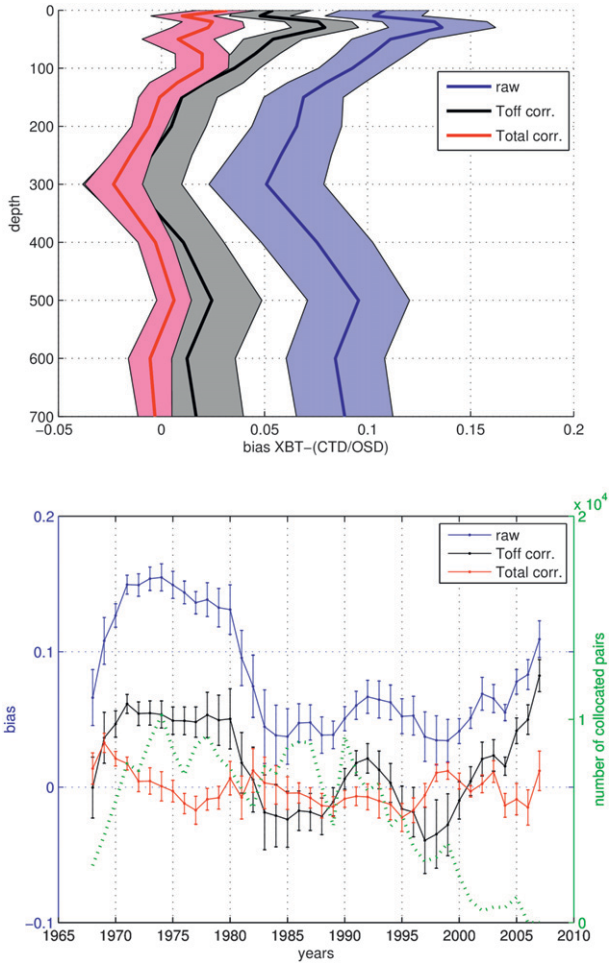


FIG. 8. (top) Profiles of median raw bias (blue), corrected by the thermal offset (black) and by a parabolic correction added to an offset (red) as a function of depth averaged over the study period 1968–2007 [curve (average) with the color band corresponding to range of one std dev of the time series variability at each depth]. (bottom) Time series of vertically averaged bias [curve (average) with vertical bars (range of one vertical std dev)]. Dashed green curve (right scale) for the number of collocated profiles. Units: °C.

estimates were not statistically significant) is also much smaller there than in other regions.

## 6. Implications of the correction approach for heat content

Figures 8, 9 illustrate the raw median bias, the bias corrected with only the thermal correction [Eq. (1)], and the bias corrected with the depth + thermal correction [(1) + (2)]. Not only is the time-averaged residual bias profile rather small (within ±0.02°C at all depths), but its time variability shows that the technique is rather good for all times and depths with biases rarely exceeding 0.05°C. This is not due to overfitting, although in the last 5 yr the number of collocated pairs starts to be too small. These figures illustrate that we have removed average biases in the collocated XBT profiles, but our method selected only a small part of the entire database (about 10%). As we do not know if this sample is representative of the whole dataset, there is no guarantee that this can be extrapolated to the remaining 90% of the profiles.

Following Wijffels et al. (2008) and Levitus et al. (2009), we also estimated a median depth bias on mechanical bathythermographs (MBTs). Using the same methodology, we performed a second-order correction added to an offset. We also separated MBT deployed at high and low temperatures. For those probes, the selected threshold was 12°C for the median temperatures calculated between the surface and 100-m depth.

With the globally corrected database, we map the observations on a latitude and longitude grid (4° × 8 The annual mean anomalies of temperature are obtained by subtracting individual data from the WOD2005 monthly climatology (Locarnini et al. 2006), and arithmetically averaging all the anomalies within each box. In a given year, we assigned to empty boxes the value of the annual mean anomaly of all full boxes for that year. Except after 2002, if Argo float profiles are included. The majority of boxes are empty (Fig. 10, bottom panel), except after 2002, if Argo float profiles are included. If only XBTs are included, less than 40% of boxes have data except in the 1990s (and a large portion of the empty boxes are in the Southern Hemisphere, in particular in the Southern Ocean).

The 0–700-m integrated heat content calculated from the corrected XBT database (green curve in Fig. 10, top panel) presents large differences from IHC from the original XBT database (red). This confirms that the local warming in the 1970s was an artifact of the positive biases in XBT temperatures (as in Domingues et al. 2008; Ishii and Kimoto 2009; Levitus et al. 2009; W08; GR10). Furthermore, we note that IHC calculated from corrected XBTs is very close to IHC calculated with the corrected data in WOD2005 (excluding Argo profiler and mooring data; such agreement is also found when considering specific layers like 0–400 or 400–700 m), whereas there were large differences between IHC from the uncorrected XBTs and from the entire uncorrected dataset. This indicates that our correction estimated with the subset of XBT profiles that could be collocated with the CTD–bottle casts holds for the entire database, at least to estimate vertically–spatially integrated variability.

Our time series of IHC (since 1970) is closest to the one from Levitus et al. (2009) and less close to IHC from Ishii and Kimoto (2009), Domingues et al. (2008) (Fig. 10, middle panel), or to GR10. However, all the time series present some similarities, despite large differences in how the data are corrected and how they are combined to provide an ocean heat content time series. The results

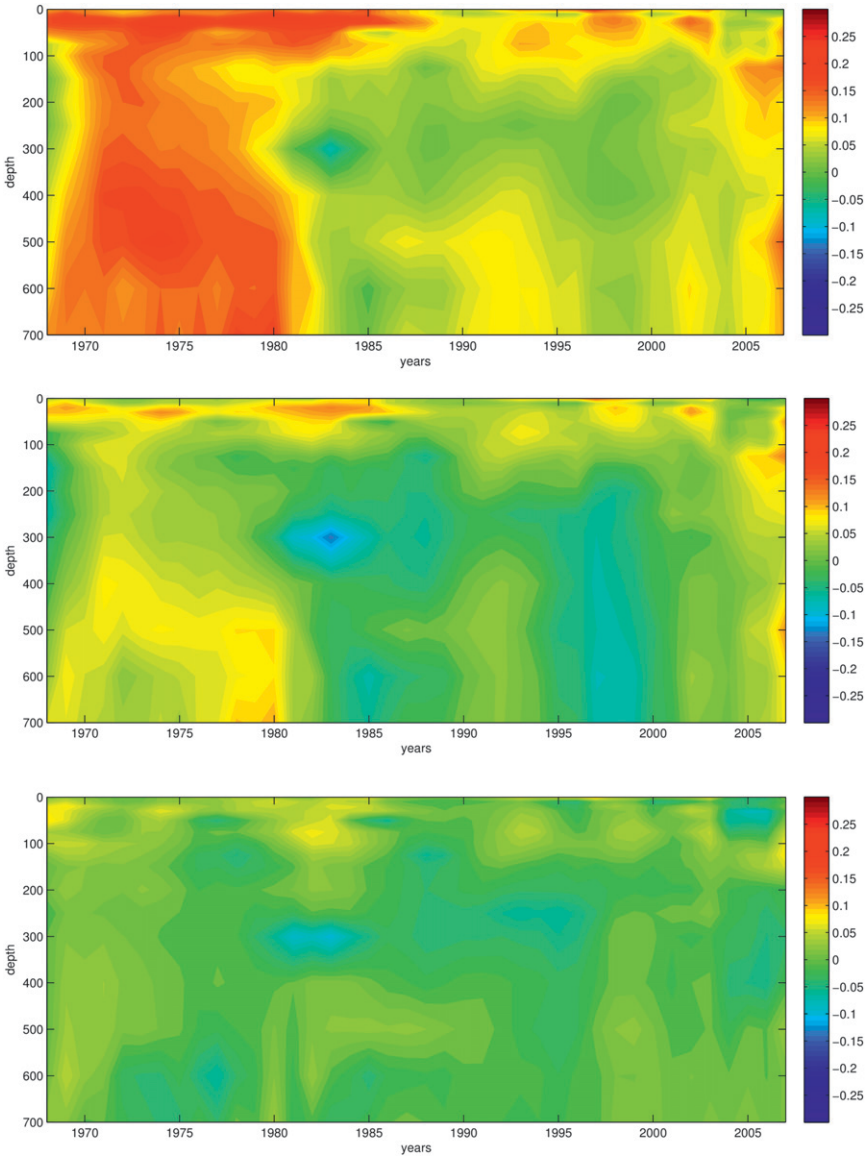


FIG. 9. (top) Evolution of XBT − CTD median raw bias, (middle) corrected by the thermal offset and (bottom) corrected by a parabolic correction added to an offset as a function of depth and time. Units: °C.

are, however, quite sensitive to insufficient sampling: for example, the large difference after 2002 between the blue curve in the upper panel and the one in the middle panel is related to the incorporation in the latter of the much better sampled Argo data. The new correction results in a linear trend for IHC of $0.39 \times 10^{22}$ J yr$^{-1}$ between 1970 and 2008 ($0.44 \times 10^{22}$ J yr$^{-1}$ without the Argo and mooring data for recent years). These are rather different from the trends for IHC for WOD2005 without correction ($0.48 \times 10^{22}$ J yr$^{-1}$). This is larger than for Ishii and Kimoto (2009; $0.27 \times 10^{22}$ J yr$^{-1}$ in 1970–2008), but less than in Domingues et al. (2008; $0.5 \times 10^{22}$ J yr$^{-1}$ in 1970–2002). The estimated IHC is strongly dependent on the assumption of filling missing boxes with the annual anomaly for that year, as many Southern Hemisphere boxes were not sampled in the early periods. There are larger differences in IHC variability with the other estimates before 1975, but data coverage starts to be really insufficient for that period.

## 7. Conclusions

We considered six different XBT classes to compute a global second-order depth correction. We chose to

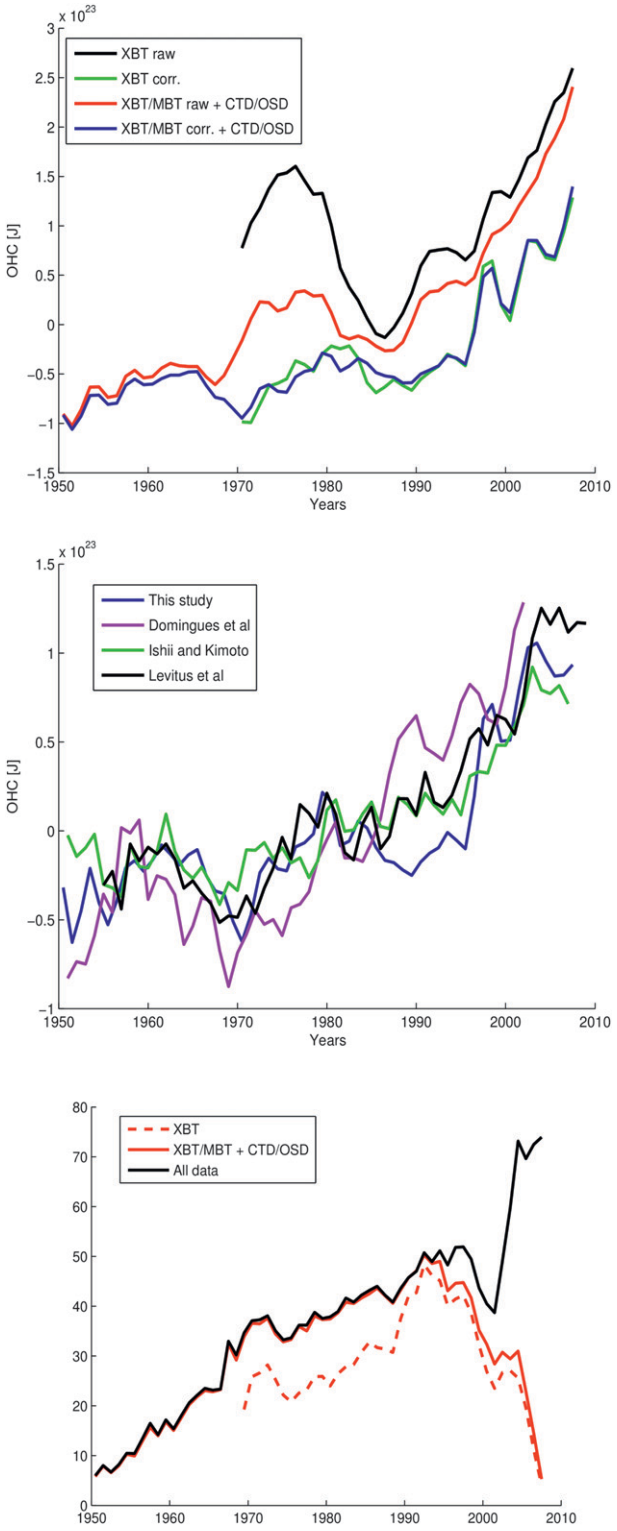


FIG. 10. (top) IHC integrated between the surface and 700-m depth calculated using the entire raw dataset (red), the entire corrected dataset excluding Argo floats (blue), and only raw XBTs (black) and corrected XBTs (green) [the average seasonal cycle from Locarnini et al. (2006) was removed from the gridded data]. (middle) IHC time series from different studies, including one for the entire corrected dataset including Argo floats (blue); the time series are reported relative to their respective time average. (bottom) Percentage of the oceanic volume covered by 4° × 8° boxes including XBT data (dotted line), all WOD2005 data (solid black line), or WOD2005 data with the exclusion of Argo and mooring data (solid red line).

separate XBTS and XBTD mostly related to T4 and T7 during the study period. We also separated XBTs deployed in cold or warm water (colder or warmer than 10°C on average between the surface and 200 m) because of the dependence on temperature of the behavior of the XBT fall rate. A parabolic correction was not sufficient, and it was necessary to apply offsets: only one thermal offset depending on the XBT type applied to the temperature profiles and a depth offset. Both are estimated in the upper layer. We also found that the results are sensitive to the choice of maximum difference of oceanic depth between collocated profiles or to criteria on minimal thermal gradients [here the thermal offset is estimated with a thermal gradient lower than 0.0025°C $m^{-1}$, whereas the upper limit is 0.005°C $m^{-1}$ in Gouretski and Reseghetti (2010)]. Although our goal was to produce global estimates, large residual biases induced us to treat separately the XBTs launched in the western Pacific basin between 1968 and 1985. This specific situation has also been discussed in W08 based on the depth error at 400 m.

This specific western Pacific correction, but also some of the time variations of the different corrections applied, illustrate that the XBT dataset in WOD2005 presents basically unexplained biases that need to be corrected empirically. The method used for these corrections, unfortunately, influences the vertical or spatial structure of the low-frequency variability portrayed by these data. What we propose is a set of corrections among other possible corrections. The separation into only two temperature categories for the depth correction equation is obviously an oversimplification, as illustrated in GR10. However, there are not enough collocated data to further investigate this temperature dependency for the depth correction on an annual basis. An alternative would be to estimate the average temperature dependence as done in GR10, but still accept a time variability of the depth correction. We also are aware of documented biases that affect specific types of probes (e.g., Kizu et al. 2011) and we did not take that into account. Clearly, the corrected dataset will thus retain spatially/time-varying biases.

Although the mode of correction of the data strongly differs between different published studies, they exhibit

similarities in the portrayed vertically integrated heat content variability. However, because of the differences in the methods applied, we expect larger differences when considering the vertical structure of the variability. For example, W08 do not use a thermal offset, and thus there is little correction near the surface. GR10 do not use a time-varying depth correction equation, and thus their estimates of thermal offset are at times rather different from ours, in particular for deep-reaching XBTs.

We corrected the MBT database with the same methodology to obtain an entire corrected database. We were able to compute a revised 0–700-m spatially integrated heat content and a corresponding new estimate of its linear trend over time. These calculations support the result of other recent papers that the anomalous increase of IHC during the 1970s originated from uncorrected XBT biases. The spatially integrated results are very sensitive to insufficient sampling (in particular in the Southern Hemisphere), as illustrated by the change in integrated ocean heat content (0–700 m) after 2002 when adding the Argo float data. Thus, the different mapping methods used to estimate IHC by different authors certainly result in large differences in IHC time variability [see, e.g., the discussion based on synthetic data in Lyman and Johnson (2008)].

*Acknowledgments.* We thank Karina Von Schuckmann, Clement de Boyer Montegut, and Cécile Cabanes for useful comments and discussions during the preparation of this manuscript, as well as the reviewers for their thoughtful comments that contributed to clarifying the manuscript. Mathieu Hamon's work is funded by IFREMER and Meteo France as part of a Coriolis Ph.D. grant. Coriolis is a joint infrastructure of IFREMER, INSU, IRD, and SHOM. The research leading to these results has received funding from the European Community's Seventh Framework Program FP7/2007-2013 under Grant Agreement 218812 (MyOcean).

## REFERENCES

DiNezio, P. N., and G. J. Goni, 2010: Identifying and estimating biases between XBT and Argo observations using satellite altimetry. *J. Atmos. Oceanic Technol.,* **27,** 226–240.

Domingues, C. M., J. A. Church, N. J. White, P. J. Gleckler, S. E. Wijffels, P. M. Barker, and J. R. Dunn, 2008: Improved estimates of upper-ocean warming and multi-decadal sea-level rise. *Nature,* **453,** 1090–1093, doi:10.1038/nature07080.

Good, S. A., 2011: Depth biases in XBT data diagnosed using bathymetry data. *J. Atmos. Oceanic Technol.,* **28,** 287–300.

Gouretski, V., and K. Koltermann, 2007: How much is the ocean really warming? *Geophys. Res. Lett.,* **34,** L01610, doi:10.1029/2006GL027834.

——, and F. Reseghetti, 2010: On depth and temperature biases in bathythermograph data: Development of a new correction scheme based on analysis of a global ocean database. *Deep-Sea Res. I,* **57,** 812–833.

Hanawa, K., P. Rual, R. Bailey, A. Sy, and M. Szabados, 1995: A new depth-time equation for Sippican or TSK T-7, T-6 and T-4 expendable bathythermographs (XBT). *Deep-Sea Res. I,* **42,** 1423–1451.

Ishii, M., and M. Kimoto, 2009: Reevaluation of historical ocean heat content variations with time-varying XBT and MBT depth bias corrections. *J. Oceanogr.,* **65,** 287–299, doi:10.1007/s10872-009-0027-7.

Kizu, S., C. Sukigara, and K. Hanawa, 2011: Comparison of the fall rate and structure of recent T-7 XBT manufactured by Sippican and TSK. *Ocean Sci.,* **7,** 231–244.

Levitus, S., J. I. Antonov, J. Wang, T. L. Delworth, K. W. Dixon, and A. J. Broccoli, 2001: Anthropogenic warming of Earth's climate system. *Science,* **292,** 265–270, doi:10.1126/science.1058154.

——, ——, and T. Boyer, 2005: Warming of the world ocean, 1955-2003. *Geophys. Res. Lett.,* **32,** L02604, doi:10.1029/2004GL021592.

——, ——, ——, R. A. Locamini, H. E. Garcia, and A. V. Mishonov, 2009: Global ocean heat content 1955-2008 in light of recently revealed instrumentation problems. *Geophys. Res. Lett.,* **36,** L07608, doi:10.1029/2008GL037155.

Locarnini, R. A., A. V. Mishonov, J. I. Antonov, T. P. Boyer, and H. E. Garcia, 2006: *Temperature*. Vol. 1, *World Ocean Atlas 2005,* NOAA Atlas NESDIS 61, 182 pp.

Lyman, J. M., and G. C. Johnson, 2008: Estimating annual global upper-ocean heat content anomalies despite irregular in situ ocean sampling. *J. Climate,* **21,** 5629–5641.

Reseghetti, F., M. Borghini, and G. M. R. Manzella, 2007: Factors affecting the quality of XBT data - results of analyses on profiles from the Western Mediterranean Sea. *Ocean Sci.,* **3,** 59–75.

Reverdin, G., F. Marin, B. Bourles, and P. L'Herminier, 2009: XBT temperature errors during French research cruises (1999–2009). *J. Atmos. Oceanic Technol.,* **26,** 2462–2473.

Roemmich, D., and B. Cornuelle, 1987: Digitization and calibration of the expendable bathythermograph. *Deep-Sea Res. I,* **34,** 299–307.

Seaver, G. A., and S. Kuleshov, 1982: Experimental and analytical error of the expendable bathythermograph. *J. Phys. Oceanogr.,* **12,** 592–600.

Thadathil, P., A. K. Saran, V. V. Gopalakrishna, P. Vethamony, N. Araligidad, and R. Bailey, 2002: XBT fall rate in waters of extreme temperature: A case study in the Antarctic Ocean. *J. Atmos. Oceanic Technol.,* **19,** 391–396.

Wijffels, S. E., J. Willis, C. M. Domingues, P. Barker, N. J. White, A. Gronell, K. Ridgway, and J. A. Church, 2008: Changing expendable bathythermograph fall rates and their impact on estimates of thermosteric sea level rise. *J. Climate,* **21,** 5657–5672.

Willis, J. K., J. M. Lyman, G. C. Johnson, and J. Gilson, 2009: In situ data biases and recent ocean heat content variability. *J. Atmos. Oceanic Technol.,* **26,** 846–852.